Neurocomputing 407 (2020) 246–258

Contents lists available at ScienceDirect

Neurocomputing

journal homepage: www.elsevier.com/locate/neucom

Neuromorphic approach to tactile edge orientation estimation using spatiotemporal similarity

Deepesh Kumar [a,*], Rohan Ghosh [a], Andrei Nakagawa-Silva [b], Alcimar B. Soares [b], Nitish V. Thakor [a,c]

[a] The N.1 Institute for Health, National University of Singapore, Singapore 117456, Singapore
[b] Faculty of Electrical Engineering, Federal University of Uberlandia, Uberlandia 38400-902, Brazil
[c] Department of Biomedical Engineering, The Johns Hopkins University, Baltimore, MD 21218, USA

ARTICLE INFO

Article history:
Received 4 June 2019
Revised 19 March 2020
Accepted 27 April 2020
Available online 13 May 2020
Communicated by Arfan Ghani

Keywords:
Tactile sensing
Neuromorphic
Biomimetic
Spatiotemporal
Edge orientation estimation
Mechanoreceptors

ABSTRACT

Moving a finger around the boundary edge is one of the important strategies followed by humans for ascertaining the shape and size of an object by touch. Tactile response from thousands of mechanoreceptors in the human hand offers a high spatiotemporal resolution to perceive the edge orientation quickly (< 50 ms) and accurately (acuity of $< 3°$). Inspired by the computational efficiency of biological tactile system, we present a neuromorphic approach to artificial tactile sensing that mimics the spike-based spatiotemporal tactile response of Fast Adapting type I (FA-I) mechanoreceptors. We propose a novel, model-based spatiotemporal correlation matching method to estimate the orientation of the boundary edge while a piezoresistive tactile sensor array attached to robotic arm palpates over the object. Results highlight the ability of the proposed method to efficiently leverage spatial and temporal information, by obtaining very precise orientation estimates ($\pm 1.67°$ error for edges oriented from 10° to 90°, with a step of 5°) in spite of a low-resolution sensor (169 mm^2, 4×4 resolution). A comparison with both spatial and spatiotemporal based classifiers indicates that the proposed method achieves 20% lower mean absolute error (MAE) than its closest counterparts, all of which required supervised training. Furthermore, we show that even with a ten-fold loss of spike time precision (1 ms–10 ms), MAE is maintained at 2°. This work highlights that even with a modest sensor size and resolution, spatiotemporal similarity metrics can be used to obtain very precise estimates of orientation. Such an approach has potential applications towards improving the tactile sensing capability in robotic/prosthetic hands where knowledge of spatial edge orientation information is paramount for object manipulation, and sensor contact area is often sparse and small.

1. Introduction

While performing activities of daily life, we often indulge in both simple touch and grasp as well as complex palpation or object manipulation tasks using our hands. Due to the high spatiotemporal resolution offered by thousands of tactile afferents (mechanoreceptors) in the glabrous skin, we can effortlessly encode and decode various tactile streams from the fingertip to perceive the salient features of an object, such as edge, curvature, roughness, etc. [1]. Fast and accurate perception of such features helps us to grasp and manipulate an object in a real environment efficiently. Since humanoid robots equipped with hands and fingers and prosthetic hands mimicking anthropomorphic design are becoming common in our daily work and social environments, it would be reasonable for such devices to emulate human tactile sensing ability. Among various senses, visual augmentation in the robotic systems has long been researched [2]. However, robotic hands hitherto have been equipped with only very limited tactile capability [3]. None of the artificial tactile sensing systems incorporated in the current robotic/prosthetic hands can match the human level of tactile sensing. Therefore, there is a need to shift research towards understanding the biological way of sensing and processing so that complex tasks of palpation and manipulation can be accomplished.

Neurophysiological studies indicate that the temporal structure of spike trains (sequence of action potential over time) generated by the population of tactile afferents serve as a neural code that helps our brain to process tactile information rapidly [4,5]. Among the four different types of mechanoreceptors, Meissner corpuscles, also known as fast adapting type-1 (FA-1) and Merkel cell, also known as slow adapting type-1 (SA-1) are particularly important for extracting fine spatiotemporal details of touched objects [6].

* Corresponding author.
E-mail address: deepeshkumar.durg@gmail.com (D. Kumar).

https://doi.org/10.1016/j.neucom.2020.04.131
0925-2312/

FA-1 afferents have the highest density at the fingertip with overlapping receptive fields which often produce population response in a particular order as the skin deforms upon contact [1,7]. It has been shown that when we touch an object, the contact information is precisely encoded in the timing and sequence of spikes, forming spatiotemporal patterns that signals the presence of various geometrical features, such as edge, curvature, texture etc., of touched object [5,7]. The sparsity offered by spike-based encoding of spatiotemporal response originating from mechanoreceptors helps the biological tactile system in fast communication and process information rapidly.

Inspired by the computational efficiency of biology, encoding of tactile information as a series of "neuromorphic" spike trains to mimic the mechanoreceptors' response characteristic has gained an appeal for artificial tactile sensing. Neuromorphic tactile sensing has shown its potential for developing neural interfaces to provide tactile feedback to amputees using upper limb neuroprosthesis [8–10]. Also, for neuro-robotic applications, neuromorphic tactile sensing has been used for differentiating various indentation conditions [11], classifying different textured surfaces [11–15] and modulating prosthesis grip control [16]. Similar to the texture, edge detection is another tactile discrimination task that helps us during object manipulation. Specifically, edge detection is the basis for contour following which help us in detecting shape of an object by palpation [17]. Therefore, edge is considered as one of the most salient features for detecting the shape of an object [18]. Daily activities that require fine manipulation, such as tying shoelaces, buttoning a shirt, and finding a coin inside a pocket, are heavily dependent on finding the edge and orientation of the object. Despite the importance of edge detection for object manipulation tasks, it has received less attention in artificial tactile sensing for robotics. One possible reason for this could be that edge related information is directly related to the perception of an object's shape, which is normally acquired by the camera systems augmenting the humanoid robots. However, vision-based robotics has some limitations too, arising from poor lighting condition, occlusion by other objects [19], and operations in environment such as underwater where vision-based sensing may simply not be possible [20]. In such scenarios, edge related tactile information may prove to be crucial for palpation and complete shape perception of an object.

The traditional approach for edge detection in tactile sensing was based on converting the response of tactile sensor array in the form of tactile image where intensity of each sensing element (taxel) was dependent on the amount of pressure applied to that taxel. Subsequently, conventional vision-based edge operators was used to extract the edge information from the tactile images [19,21]. However, unlike a vision sensor, the tactile sensor needs physical contact with the object. Therefore, the tactile images obtained from the deflection of the contact surfaces adds extra noise to the tactile image compared to the visual image. Also, the resolution of tactile sensors is generally much less than the vision sensor and uncertainty is added in the tactile response due to deformation of the elastic medium of many objects being manipulated or the softness of the prosthetic finger during palpation or manipulation. Due to such issues in tactile sensing, the conventional vision-based approach for edge detection might not perform as expected [22]. Therefore, we hypothesize that inspiration from human tactile sensory system may provide alternatives ways for tactile edge orientation estimation. Recently, Pruszynski et al. [5] conducted a neurophysiological study with human participants to show that the first order tactile neurons such as SA-I and FA-I in the human fingertip signals edge orientation via the spatiotemporal structure of their tactile responses. In another study [23] authors recorded spike-trains generated by the overlapping receptive fields of FA-I and SA-I neurons and reported that humans could distinguish the edges spanning the entire fingertip with 3° of edge orientation resolution.

Based on neurophysiological studies [5,23] highlighting tactile edge orientation processing by first order tactile neurons, we developed a neuromorphic approach to tactile sensing in robotics for estimating tactile edge orientation. Unlike the study presented by Rongala et al. [24] for bio-mimetic approach for tactile edge orientation estimation, in this study we use active palpation to estimate the edge orientation. Also, we present a simpler approach that uses tactile response from the group of first order neurons to find the spatiotemporal similarity corresponding to different edge orientations. Our system consists of a piezoresistive tactile sensor array attached to the robotic end-effector, an interface that produce spike trains to mimic neural signal from mechanoreceptors [7], and a computational model to analyze spiking activity for estimating edge orientation. There exists spike train metrics (e.g., Victor-Purpura [25] and Van Rossum [26] spike distances) that can be used to find the similarity between two spike trains. Such spike train metrics have been used by Zhengkun and Yilei [15] and Rongala et al. [27] for surface texture classification using single-unit spike train. However, in this study, to decode the orientations of edge that traverse through all the taxels of the sensor, we need to consider the group of spike trains (16 spike trains for this study) over the entire palpation duration. Computing pairwise spike distances between a group of 16 spike trains of one edge orientation with every other orientation are computationally exhaustive. Also, spike distance metrics are generally used for the analysis of temporal coding [28], however, here, depending on the orientation of edge, different taxels of the tactile sensor may produce variable firing rates (rate coding).

In this study, we propose a novel computational method based on spatiotemporal-correlation matching for edge orientation estimation. The proposed spatiotemporal correlation metric, weighted spatiotemporal similarity (WSS), uses spatial pattern information and its temporal evolution for orientation estimation. This method leverages the entire tactile information obtained across the duration of palpation, for more accurate estimation of edge orientation. Further, WSS uses normalized tactile images for computing correlation, which by definition renders it partially invariant to absolute pressure magnitude.

The rest of this paper is organized as follows. Section 2 provides a detailed description of materials and methods that includes sensor design, experimental setup, neuronal models and edge orientation estimation algorithm. Section 3 provides our results and major findings. Finally, in Section 4 and 5 we present the discussion and concluding remarks, respectively.

2. Materials and methods

2.1. Tactile sensor

In this study, we custom-built a 4 × 4 (active area = 13 × 13 m m) piezoresistive tactile sensor array. A piezoresistive cloth is sandwiched between two layers of conductive traces arranged as rows and columns (Fig. 1(a)). The contact between the cloth, the rows, and the columns constitutes a sensing element denominated as a taxel. Traces are 2 mm wide and separated by 1 mm arranged in the form of 4×4 matrix i.e., total of 16 taxels (Fig. 1(b) and (c)). The size of the sensor is suitable for mounting it on the fingertip of the robotic/prosthetic hand. The tactile data were recorded using a data acquisition board (DAQ) which sampled each taxel individually at 1 kHz per taxel. The DAQ board contains an ARM Cortex-M3 microcontroller and communicates with the computer system via USB communication at Full-Speed with each individual taxel being sample at a frequency of 1000 Hz. Analog circuitry consists

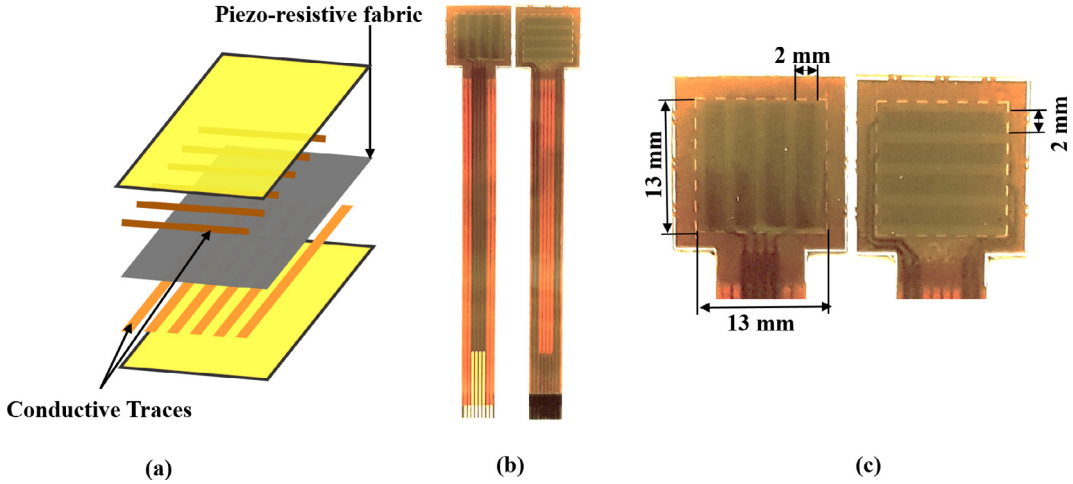

Fig. 1. (a) Fabrication principle of the 4 × 4 tactile sensor array. (b) Full view of the custom-built 4 × 4 tactile sensor array. (c) Enlarged view of the tactile sensor showing the row and column traces. The effective sensing area of tactile sensor is of 13 mm × 13 mm and each row and column traces are of 2 mm width.

of multiplexers and single pole double throw (SPDT) switches for controlling the read-out procedure of each taxel of the tactile sensor array. The firmware makes use of Direct Memory Access to drastically improve the speed of ADC conversion and makes use of the full capacity of the USB communication speed.

2.2. Robotic platform and tactile stimulus

As shown in Fig. 2(a), we mounted our tactile sensor to a customized 3D printed end-effector and attached it to the arm of UR-10 robot (Universal Robots, Denmark). A 1 mm thick skin-like soft layer made by molding a polymeric viscous material (Dragon Skin 30, smooth on USA) was used to cover the sensor. The soft layer provided increased friction during palpation and also offered compliance property to the tactile sensor, analogues to the human fingertip.

A customized robotic end-effector was used to perform active palpation over the tactile stimulus for detecting the edge orientation. By active palpation we mean that the tactile stimulus was fixed on the table surface whereas the tactile sensor attached to a robotic end-effector palpated over the tactile stimulus. The tactile stimulus used in this study was a rectangular object of height 1 cm, length 20 cm, and width 5 cm, and it was firmly attached to the top of the table as shown in Fig. 2(b). The tactile stimulus had a plane surface and we were interested to estimate the orientation of the boundary edge of rectangular object when tactile sensor attached to a robotic end-effector palpated from point $P1$ to $P2$, as shown in Fig. 2(b). Point $P1$ was always inside the plane surface of object and point $P2$ was always kept outside the object (in the air). As robotic end-effector palpated from $P1$ to $P2$, at the transition point from plane surface to outside of object, tactile sensor palpated over the boundary edge of tactile stimulus. The tactile stimulus was placed on the table at 17 different orientations from 10° to 90° with a step of 5°, as shown in Fig. 2(c). Note that, the sensor orientation and palpation direction was kept constant at all time, and orientation of an edge was measured as the angle between the line parallel to the tactile sensor's horizontal axis and rectangular object's long side, as shown in Fig. 2(c).

2.3. Experimental protocol

Fig. 2 shows the experimental setup used in this study. The palpation experiment started by positioning the tactile sensor attached to a robotic end-effector at 10 mm above the tactile stimulus surface. Then the robotic end-effector was slowly moved down (negative z-axis) until the tactile sensor made contact with the plane surface of the tactile stimulus and all the taxels of sensor array got activated. The initial point of contact ($P1$) between sensor and object surface was chosen in such a way that none of the taxels was at boundary edge of the object. The robotic end-effector was maintained at $P1$ for 2 s, and then the tactile sensor started palpation by moving the robotic end-effector towards point $P2$ located at the outside of object (Fig. 2(b)). During the palpation, the tactile sensor palpated over the edge at the transition point from inside the object's surface to outside the object, and we aimed to estimate the orientation of that boundary edge. We chose the palpation speed as 2 mm/s as an initial approximation, however it can be changed depending on the experimental design condition. At the end of palpation, the robotic end-effector was kept still for 2 s before the whole palpation process repeated. For each angle of edge orientation (from 10° to 90° with an incremental step of 5°), the palpation experiment was repeated for ten trials. During palpation, the tactile response from the 4x4 tactile sensor array was recorded for offline processing.

2.4. Spiking neuron model

Spiking neuron models are used to convert the analog response obtained from the sensor into train of spike events that mimic the communication principle followed by biological neurons, i.e., spike-based encoding and decoding of sensory information. There are many spiking neuron models proposed by neuroscientists that convert analog signals into spike trains [29–31]. In this study, we used the well-established Izhikevich neuron model [32] that strikes a trade-off between the Hodgkin Huxley model [30], that is bio-physically accurate but computationally prohibitive, and the integrate-and-fire model [31], that is computationally efficient but limited in generating rich spiking pattern. The Izhikevich model has been used extensively for mimicking the firing behavior of mechanoreceptors by different researchers [11,33–35].

Here we chose to encode analog tactile signal into spike trains that mimics FA-I mechanoreceptors firing behaviour. This is because, among different mechanoreceptors, FA-I is known to encode the sudden change in pressure for enhanced representation of local spatial discontinuity [7] and edge is nothing but the local spatial discontinuity that occurs at the boundary of two adjacent regions which is different from one another. Since in our current study, we aimed to detect the boundary edge of an object which

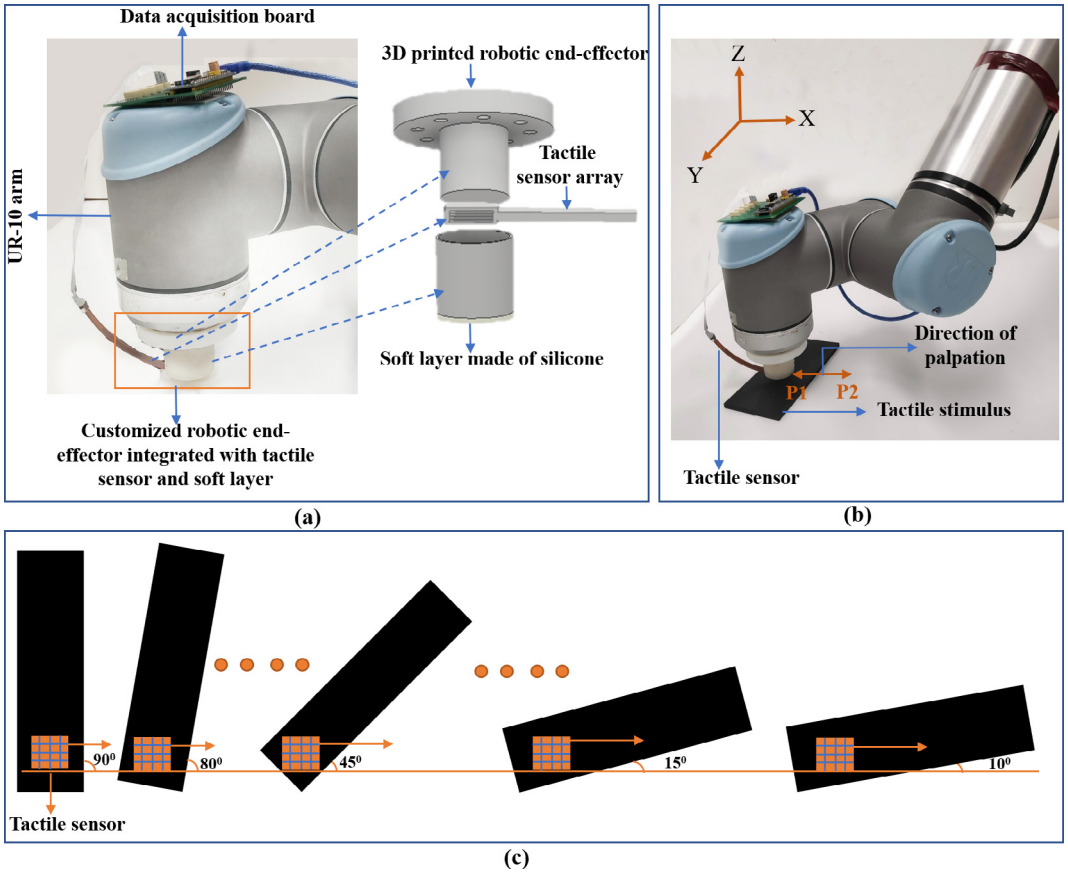

Fig. 2. Experimental setup (a) Customized robotic end-effector to perform palpation procedure. The tactile sensor was pasted to a 3D printed structure attached to the UR-10 arm, and a sleeve of the soft layer (2 mm thickness at the bottom) was used to cover the sensor. (b) A tactile sensor positioned at the initial point of contact P1 at the flat surface inside the tactile stimulus. Robot palpates from point *P*1 to *P*2 (that lies outside the object) while passing through the object's boundary edge. (c) The tactile stimulus was a rectangular object that was placed at 17 different angles of orientation, starting from 90° to 10° with an intermediate step of 5°. The angle of edge orientation was measured between the line parallel to the horizontal axis of the tactile sensor and the long axis of the tactile stimulus.

resembles a sharp local spatial discontinuity, it was reasonable to mimic the firing behavior of FA-I receptor to encode the edge information. The Izhikevich neuron model [32] is described by following differential equations:

$$\frac{dv}{dt} = 0.04v^2 + 5v + 140 - u + I \tag{1}$$

$$\frac{du}{dt} = a(bv - u) \tag{2}$$

where v stands for membrane voltage and u stands for membrane recovery variable, and I is the input current that excites the neuron. Variables a, b, c, d in Eq. (1) and (2) are the standard parameters used in the Izhikevich neuron model. In order to reproduce the spiking behavior of FA-I afferents, we have used the following values for the parameters: $a = 0.02, b = 0.2, c = -65$ and $d = 2$ [32]. The parameter a determines the decay rate, b controls sensitivity to spikes, c regulates membrane reset voltage, and d governs reset value of the adaptation variable. Whenever the membrane potential v is driven to threshold $v = 30$ mV, a spike is produced, and the after-spiking reset is triggered.

$$\text{if } v \geqslant 30\,\text{mV}, \quad \text{then } \begin{cases} v \leftarrow c \\ u \leftarrow u + d \end{cases} \tag{3}$$

Since FA-I receptors respond to a sudden change in the pressure level at the skin, it is convenient to derive the virtual current for simulating the FA-I response as derivative of the analog tactile response. Therefore, the output of the tactile sensor was first normalized, and then the absolute of derivative of normalized tactile response (V) was fed as a virtual current (I_{FA}) to the Izikevitch neuron model (Eq. 1), which generates FA-I mechanoreceptors-like spike trains.

$$I_{FA} = G * \left|\frac{dV}{dt}\right| \tag{4}$$

Fig. 3(a) shows the filtered tactile response of the tactile sensor recorded from a single taxel while the sensor array palpated over the object as explained in Section 2.3. Note that, the tactile responses from all the 16 taxels were used in this study, but for the purpose of visualization, we are only showing the response of a single taxel. The output of the piezoresistive tactile sensor had an inverse relationship with the applied pressure to it. Therefore, you can see from Fig. 3(a) that, when the tactile sensor was in direct contact with object's plane surface, the output of taxel was around 1.75 V and as the sensor started moving out of object, the amplitude of sensor output started increasing. Finally, output of sensor got saturated once the sensor moved completely out of object's surface. Fig. 3(b) shows the derived virtual input current using Eq. (4). The value of G was chosen empirically in such a way that the output spikes follow the response characteristic of FA-I mechanoreceptors. The virtual input current (I_{FA}) was fed to the Izhikevich neuron model to generate the spike trains that mimicked the firing pattern of FA-I mechanoreceptor, as shown in Fig. 3 (c). We can see that no spike events are fired corresponding to the time when the sensor was on the plane surface of the object that offered near constant pressure to the sensor. However, during

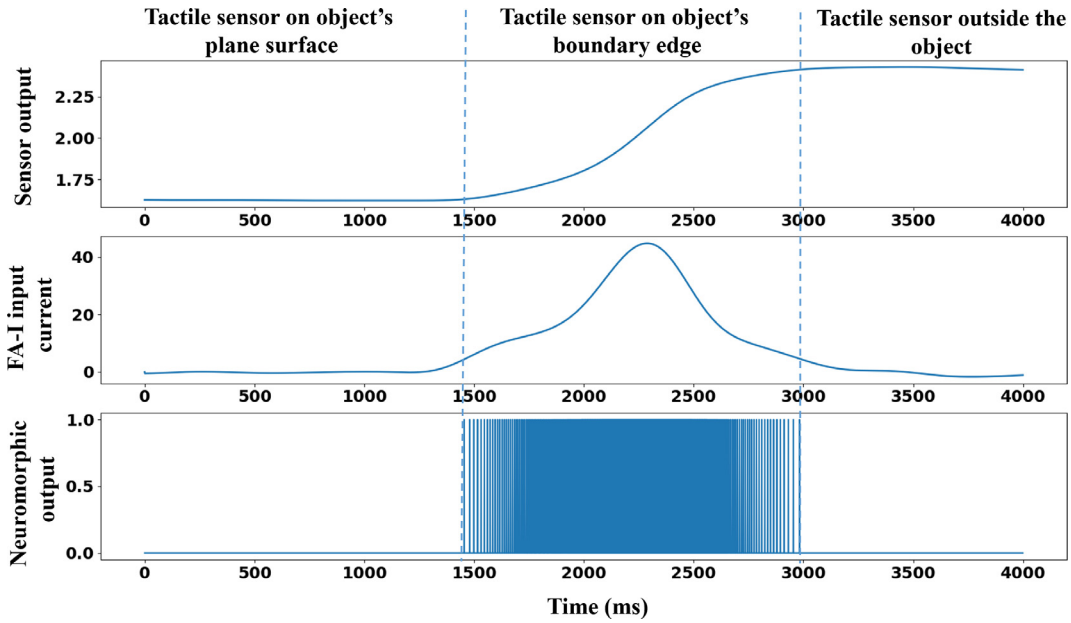

Fig. 3. (a) Raw tactile data recorded from single taxel of the 4 × 4 tactile sensor array, (b) Virtual input current fed to the Izhikevich neuron model to generate spike events, and (c) Simulated spike train that mimics the behaviour of FA-I mechanoreceptors.

the transition from the plane surface (full contact) to outside of object (no contact), there was a dynamic change in the sensor output due to local spatial discontinuity. Therefore, FA-I fired only when the sensor was palpating over the boundary edge of an object. Once the tactile sensor went off the object, simulated FA-I stopped firing.

The spikes generated by the Izhikevich model are finally denoted by the tuples $(x_i, y_i, t_i), i \in (1, N)$. The first two parameters encode the location of each spike (taxel's position on the 4x4 array), whereas the third parameter encodes the time instant (in milliseconds) at which the spike was produced. Finally, N denotes the total number of spikes recorded. The spike events were recorded separately for each of the 16 taxels.

2.5. Weighted spatiotemporal-similarity for edge orientation estimation

The objective of the steps elaborated in this section is to estimate edge orientation as the tactile sensor palpated over the object. Proceeding with the definitions made towards the end of the previous section, we first binned spikes collected from fixed windows of length T ms to form tactile images of size 4 × 4 (same as the resolution of tactile sensor). We have executed several experiments with different window length and found that $T \approx 100$ ms generates noise-free spikes from edge palpation, while accurately capturing the spatial edge pattern over time. However, to utilize temporal resolution of tactile response, we chose to have an overlap of 90 ms in the window-length for binning the spikes. The resulting tactile images (of size 4x4) are denoted as $I_0, I_1, \ldots, I_k$.

In order to estimate edge orientation from these images, we define a weighted spatiotemporal-similarity (WSS) based metric. We approach orientation estimation as a class estimation problem, where the classes are orientations $S_\theta = \{10^\circ, 15^\circ, 20^\circ \ldots, 90^\circ\}$. Denoting a class by its corresponding orientation θ, the WSS metric for θ, WSS_θ, is computed as

$$WSS_\theta(k) = \frac{\sum_{i=0}^{k(\theta)} w(i) R\left(I_{k-i}, I_i^{sim}(\theta)\right)}{\sum_{i=0}^{k(\theta)} w(i)} \quad (5)$$

$R(X, Y)$ is the Pearson's normalized correlation coefficient between images X and Y. $I^{sim}(\theta)$ are the simulated, ideal spike images obtained when an edge of orientation θ traverses the sensor. During simulation, we assumed the width of line (edge) moving across the sensor to be very small (0.2 mm). This is because, when tactile sensor palpated over the object, we considered that the edge was encountered by individual taxel of sensor when the taxel moved from inside the object's surface to outside the object , passing through infinitesimal width of boundary edge. Also, we assume that when the simulated edge stimuli traversed over the sensor, the applied force has a Gaussian distribution over the tactile sensor and thus individual taxels at location (x,y) receive a portion of the applied pressure in a distance dependent way. Therefore, the magnitude of each taxel in the simulated image was computed as

$$I_i^{sim}(\theta)(x, y) = e^{-\frac{d((l(\theta,i),(x,y)))^2}{\sigma^2}} \quad (6)$$

Here, (x,y) represent the location of taxel in the simulated image of size 4×4, d is the distance function, and $l(\theta, i)$ is the simulated line representing the edge oriented at angle θ at frame i. Unlike I, I^{sim} is ordered reverse in time, such that $I_0^{sim}(\theta)$ is the simulated image obtained when the edge has traversed to the end of the sensor. These simulated images are created by assuming the edge to be a straight line moving along the sensor at a velocity which is known beforehand and kept fixed for all experiments (see Fig. 4)

Since the tactile images were generated based on the number of spikes over a time interval, the intensity of image was dependent on the spike rate. For a taxel, ideally the spike rate should follow the Gaussian distribution having maximum spike rate when edge is within the taxel's area and decreasing monotonically both side before the edge reaches to taxel and after edge passes away from taxel. Therefore, while calculating WSS metric, it is important to consider the effect of spike rate (SR) at different times. Thus in Eq. (5), we used w(i) as a weight function which assigns a different weight to each of the correlation between the observed spike image and simulated image based on spike rate over time. $WSS_\theta(k)$ essentially then provides a correlation based metric which represents the similarity of the spike pattern obtained from the sensor, and the simulated ideal edge patterns at various orienta-

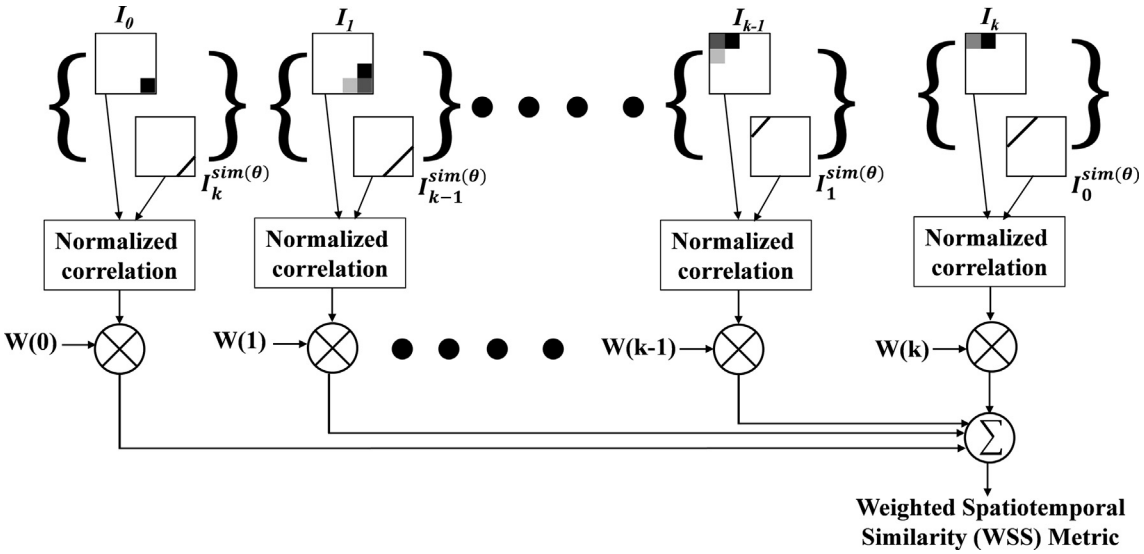

Fig. 4. Weighted spatiotemporal-correlations matching to estimate the edge orientation.

tions, at time kT ms. This metric would result in a high value when the observed data contains a traversing edge, oriented at θ, and located within the sensor area until kT ms. As we do not know when the edge leaves the sensor, this metric needs to be computed at all frames, $WSS_\theta(1), WSS_\theta(2), \ldots, WSS_\theta(k)$, and for all orientations in S_θ. The best estimate of orientation from the data, θ_{est}, can then be found as

$$\theta_{est} = argmax_{\theta \in S_\theta} (max_i WSS_\theta(i)) \quad (7)$$

However note that the above equation assumes that an edge was present in the recorded spike data, and finished its traversal within the recorded time. To handle cases where these assumptions do not apply simple thresholding on the maximum value of the similarity metric might help.

3. Results

This section presents the performance of our method in estimating edge orientation. The effect of various parameters on edge estimation accuracy is also discussed, such as the effect of palpation speed and palpation duration, robustness to spike-time noise, etc. We also compare the performance of our method with other methods to establish relevance and demonstrate the efficacy of the proposed method.

3.1. Analysis of spike-time distance distribution

First we start by analyzing the distribution of the spikes generated by an individual taxel across time. For each taxel, we centered the distribution at the time instant when the straight edge coincides with the center of the taxel. Since we knew the speed and duration of palpation over the edge, we also knew the ground truth of the edge location over the sensor at all times. This allows us to center the distribution to the time instances when the edges were directly over the center of the taxels. Further, we calculated the relative difference in time between the median position of spike train and timing of all the other spikes for that taxel (spike-time distance. The distribution was estimated by combining the spike-time distances for all the edge orientations corresponding to individual taxels. This process was repeated for all 16 taxels separately. Fig. 5 shows the distribution of spike-time distance for all the taxels.

Ideally, we expected that the tactile response of every taxel combined over all the edge orientations would follow similar distribution fit. This was expected as the palpation speed and force was constant during the experiment. However, looking at the distribution shown in Fig. 5, we see that each taxel's spiking behavior was different than others'. Also, considering the palpation speed and size of the sensor array, each taxel should be on edge for maximum of 1.5 s. Therefore, we should observe spikes up to ± 0.75 ms around the center of spike-time distance distribution. However, we see that the spike distribution has a large variance of ± 1.6. Such a large variance indicates that individual taxels started firing even before the edge entered to the taxel and continued to fire even after edge went out of the taxel. This behavior was consistent with all the taxel indicating large temporal overlap in spiking activities between neighboring taxel locations. Also, the temporal location of maximum spike-activity rarely coincides with zero, indicating that the taxels may generate maximum spikes before or after the edge centers on it. Such noisy spike generation from the tactile sensor makes this a challenging problem to fit a well-defined model using only the spatial information at a single time frame. However, we show that our proposed model that uses spatiotemporal information can be an alternative to estimate edge orientations in such cases.

3.2. Estimation of edge orientations

Here, we aimed to estimate the orientation of the boundary edge of an object among 17 different possible edge orientations (10° to 90° with a step of 5°). As per the palpation procedure adopted in this study, different taxels of the tactile sensor exit the object surface at different time instances depending on the orientation of the object. Therefore, the tactile sensor generated a sequence of tactile images of spike patterns over time that is unique to the orientation of the object's boundary edge. These tactile images were used to perform normalized correlation with the simulated images that were generated assuming the ideal tactile response by the individual taxels over time when the tactile sensor traversed through the edge of a certain orientation. The idea was to find out the orientation of the simulated images which produce the highest correlation in time with the actual tactile images obtained by palpating over the object (see Section 2.5 for details). Since the tactile images were generated based on the number of spikes, it

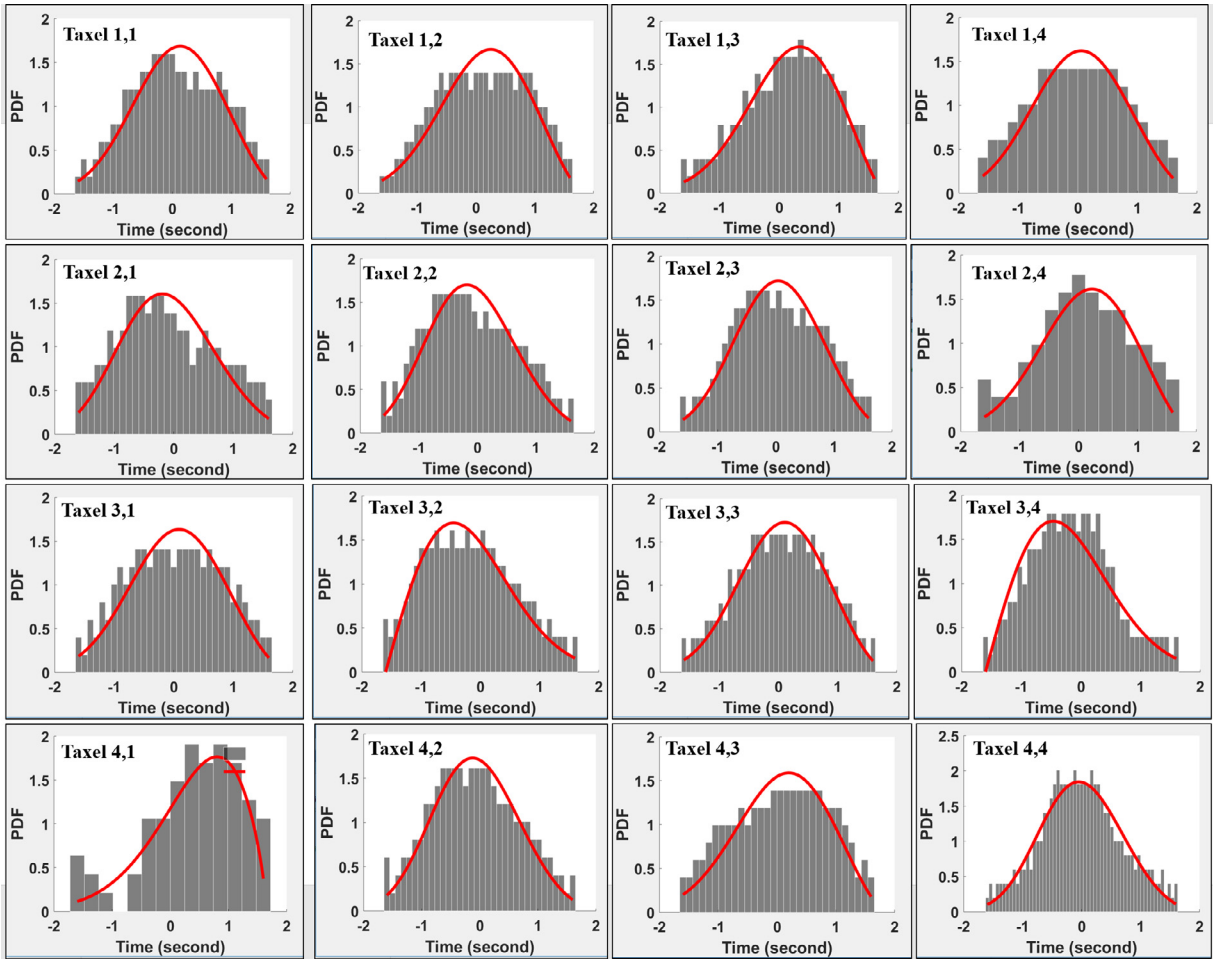

Fig. 5. Spike-time distance distribution for individual taxel combined over all the edge orientations. The red line presents distribution fit over the histogram. (For interpretation of the references to colour in this figure legend, the reader is referred to the web version of this article.)

was imperative to consider the effect of spike rate (SR) over time while calculating the WSS metric. Therefore, we explored three different choices of weight factor ($w(i)$) to maximize the performance of our method for calculating the WSS metric. Specifically, we used weight factors as $w(i)$ = constant, (1-SR) and $(1 + SR)$ during evaluating Eq. (5). We found that the choice of $w(i) = (1 - SR)$ provided the best performance for our system, and therefore all the results presented here and in the subsequent sections are based on $w(i) = (1 - SR)$.

For each orientation of edge, we computed the *WSS* metric (Eq. (5)) between the spike images generated by palpating over the edge and ideal simulated images ($I^{sim}(\theta)$) for all the possible edge orientations (total of 17 classes from 10° to 90° with steps of 5°). That means, for each edge orientation, we calculated 17 different WSS metrics corresponding to 17 different classes of possible edge orientation. Subsequently, the edge orientation corresponding to a maximum WSS_θ (Eq. (7)) was considered the actual orientation of the edge over which sensor palpated. The palpation experiment was repeated ten times for each angle of orientation.

The proposed methodology was able to estimate the edge orientation with the overall mean absolute error (MAE) of 1.67° with an acuity of 5°. However, for the acuity of 10°, we observed zero MAE. Table 1 shows the MAE obtained for estimation of individual edge orientations, and we can see that maximum observed error was limited to 5° for 40° of orientation whereas there was 0° error for five different classes of edge orientations. Also, Fig. 6 shows the confusion matrix obtained for 10 trials of each classes using

Table 1
Mean absolute error in estimated orientations of edge using WSS method.

Edge orientation	Mean absolute error	Edge orientation	Mean absolute error
10°	0°	50°	4°
15°	0°	55°	1°
20°	2°	60°	1°
25°	1°	65°	1°
30°	0°	70°	4.5°
35°	4°	75°	2.5°
40°	5°	80°	2°
45°	0°	85°	0.5°
		90°	0°

WSS-based model. We can see from the confusion matrix that, 6 classes (10°, 15°, 30°, 45°, 65° and 90°) out of 17 classes had no confusion with other edge orientations. The rest of the classes showed confusion in few trials, however, the confusion was always limited to their neighboring edge orientation (i.e. error never exceeded beyond ±5°)

To evaluate the efficacy of the proposed method, we compared the performance of WSS method with other methods available in literature. Recently, Delhaye et al. [36], and Zhao et al. [37], used feed-forward artificial neural network (ANN) as a decoding method to estimate tactile edge orientation in human fingertip. These studies were based on the neurophysiological tactile perception rather than artificial tactile sensing. Therefore, we chose a custom ANN

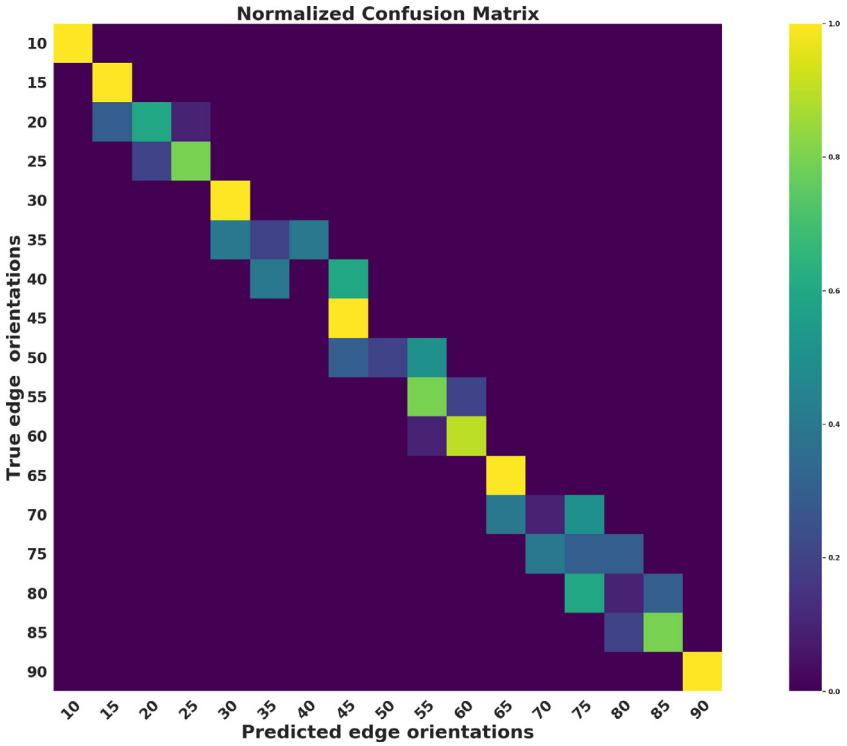

Fig. 6. Normalized confusion matrix for WSS-based edge orientation estimation. The model was tested for 10 trials of each edge orientation.

architecture as one of the method for comparison. Also, in the vision domain there exist several spike-based visual recognition method that uses spatiotemporal information. One such method is event-based deep belief network (EDBN) proposed by O'Connor et al. [38], where they classified hand written digits from MNIST dataset while using Integrate-and-fire-neuron based spike information. Since EDBN approach uses spike-based spatiotemporal data for classification, we implemented this method and compared it's performance with the proposed method in this study.

The input data fed to the ANN was either only spatial or spatiotemporal tactile images. Individual tactile images were used for input while generating orientation estimates over entire trial and orientation output was decided using winner take all approach. However, for spatiotemporal tactile input a larger input vector consisting of N consecutive tactile images was used and orientation estimates over entire trial was found out similarly using winner take all approach. The ANN architecture had single hidden layers with 30 neurons, and we prepared a spatial and spatiotemporal image database of ten trials for each edge orientations. We adopted for leave-one-out cross validation (LOOCV) approach to test the ANN method. To perform LOOCV, out of the ten trials of palpation for each orientation, we trained the network using the images of nine trial of each of the 17 orientations and tested the system with the images from remaining one trials. This process was repeated 10 times and each time leaving out a different pair to use as the single test case. For each test case, we used a winner-take-all approach to compute the final estimate of orientation from the neural network output layer. This approach involves adding the activation values of each "winner" orientation for each frame within the trial and choosing the orientation with the maximum value of the final summed activation. The EDBN network proposed by O'cornor et al. [38] used persistent contrastive divergent method [39] for training the network. Since EDBN was designed to work with the spatiotemporal data, we used only spatiotemporal spike images as input to the EDBN network. This network. To evaluate EDBN we used similar approach as was used for ANN method i.e. winner-take-all approach.

Table 2 shows the comparison of proposed method with ANN and EDBN network. We can see that the proposed method, WSS-based approach, was able to estimate edge orientation with 20% lower MAE compared to its closest counterpart i.e., EDBN method. Also, unlike EDBN and ANN, the WSS-based approach being a model-based approach does not require data for training. Therefore, it is computationally less expensive and suitable for real-time applications, though in this study the edge orientation was estimated offline. The offline processing was performed in Matlab software running on a system having Intel Core i7-6700 CPU @3. 40 GHz–3.41 GHz processor. Using the tactile data from entire duration of palpation, the orientation of an edge was estimated in 3.05 s. We can also see that the maximum MAE obtained for an edge orientation is lowest for WSS-based method (4.5° for 70° of edge orientation) compared to next best maximum MAE of 6.2° for EDBN method. Among all the methods presented here, the ANN approach which used spatial input (static input) offered the highest overall MAE of 9.13° whereas the same approach with spatiotemporal input provided MAE of 2.4°. This indicates that, using spatiotemporal tactile information has advantage over using only spatial information for estimating the edge orientations.

3.3. Effect of palpation duration over the edge

A sequence of $I_i^{\text{sim}}(\theta)$ was used to calculate the *WSS* metric starting from time kT ms (time at which tactile sensor exit the object) till the time when the first spike image (I_1) was obtained. This means that the result presented in the previous section considered all the spike events from start to end of the palpation over the edge. Here we investigate how the performance of our proposed method changes if we gradually reduce the number of spike events used to decide orientation estimation. Here, by the number of spike events, we mean that the WSS_θ is calculated for the different fraction of total palpation duration ($\Delta T = T_{\text{fin}} - T_{\text{ini}}$) over the edge. Specifically, we tested our method by taking the spike events corresponding to $0.2\Delta T$ to ΔT with a step size of 0.2. Fig. 7 shows the

Table 2
Comparison of WSS method with other networks for edge orientation estimation.

	ANN (S)	ANN (ST)	EDBN	WSS
Overall MAE (±SD)	7.61° (±7.01°)	2.25° (±2.45°)	2.2° (±2.3°)	**1.67° (±1.79°)**
Maximum MAE	14.72°	5.5°	6.1°	**5°**

Note: ANN = Artificial neural network, S = Spatial, ST = Spatiotemporal; EDBN = Event-based Deep Belief Network; WSS = Weighted spatiotemporal similarity; SD = Standard deviation; MAE = Mean absolute error.

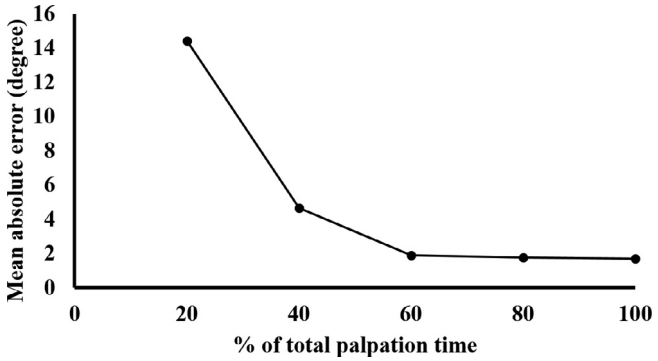

Fig. 7. Mean absolute error in edge orientation estimation (10 trials for each angle) as the number of spike-data used to estimate the orientation is reduced from spike events corresponding to 100% to 20% of total palpation duration.

performance of our method with varying palpation time, which indicates that the MAE for edge orientation estimation went on increasing as we decreased the palpation duration. This is because as we reduce the palpation duration, we continue to reduce the number of spike events to decide the edge orientations. However, looking at Fig. 7, we see that till the 60% of palpation duration, there was an insignificant increase in MAE (0.1°) compared to the MAE corresponding to 100% palpation duration. The error started increasing rapidly only after the palpation duration was reduced below 60% of total palpation duration. Thus, our proposed method is robust enough to estimate the object's boundary edge orientation even with the spike data gathered when only 60% of our tactile sensor passes over the edge.

3.4. Effect of spike-time noise on edge orientation estimation

In this section, we analyze the spike data to understand the robustness of the proposed method to noise in the timing of spike events. To do that, we added spike-time noise into the recorded spike events which randomly displaced the timing of spikes by τ ms (τ ranging from 1 ms to 30 ms). Fig. 8 showed the performance of the system when noisy data was used to estimate the edge orientations. Since the spike-time noise was added randomly, we repeated the evaluation three times to average out the variation in the obtained result. We can see from Fig. 8 that there is a visible increase in MAE for 1 ms of noise level. However, the growth in MAE does not increase to significant level until the noise level goes beyond 10 ms. This result highlights that the proposed method is sensitive to the timing of spikes as evident from the increase in the MAE by 0.23° for the noise level as low as 1 ms. At the same time increase in MAE by just 1.33° for the noise level up to 10 ms indicates that this method is robust enough to counter the moderate amount of noise in the timing of spikes for tactile perception. Such robustness is important while interacting with the real world environment where the palpation condition might not be as standard as the laboratory experiments.

3.5. Effect of sensor area on the edge orientation estimation

The tactile sensor used in this study had 16 taxels (4×4) in the effective sensing area of 169 mm^2 (13 mm $\times$ 13 mm). Earlier, we reported that we could estimate the edge orientation with overall MAE of 1.67° (for 5° of acuity) and 0° (for 10° of acuity). Here, we explored how does reducing the area of sensor, which also reduced a number of taxels (keeping the sensor resolution intact) affect the efficacy of our system in estimating the edge orientation. To understand this we considered the spike events from the sensor area having 4×4, 3×3 and 2×2 taxels as shown in Fig. 9c) and performed the edge orientation estimation process. Fig. 9(d) shows the comparison between the performance of the system corresponding to the different sensor area. Note that, the result shown in Fig. 9(d) is the average of all possible combinations of sensor area of 4×4 (1 combination), 3×3 (4 combinations) and 2×2 (9 combinations) adjacent taxels. As expected, the overall MAE

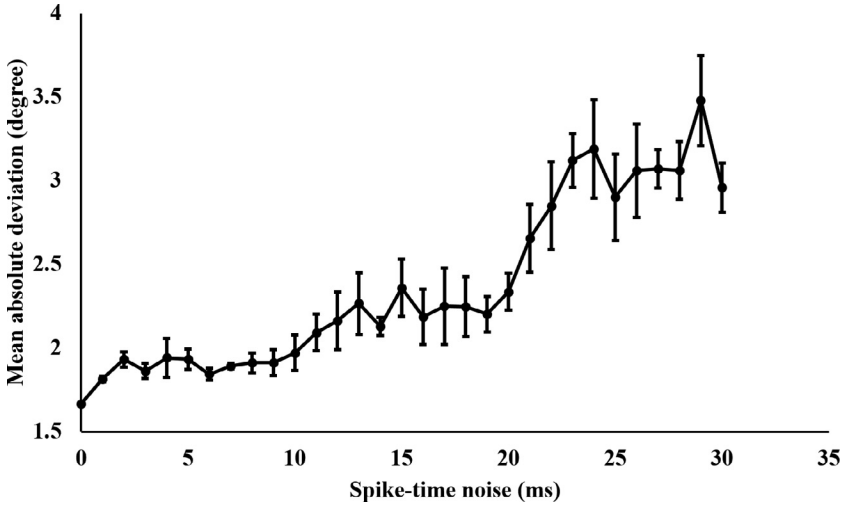

Fig. 8. Effect of adding spike-time noise (range of 2–30 ms) on edge orientation estimation error.

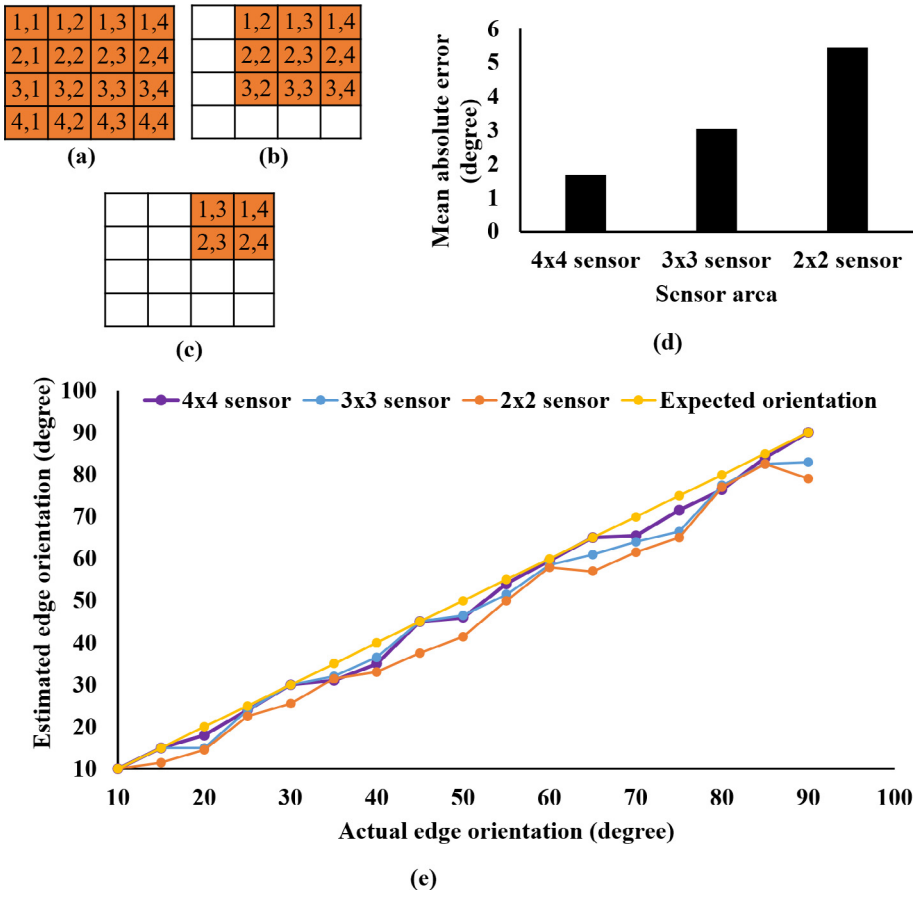

Fig. 9. (a) Tactile sensor with full area (4 × 4). (b) 3 × 3 tactile sensor. (c) 2 × 2 tactile sensor. (d) Bar graph comparing the MAE obtained by using a different area of the sensor for edge orientation estimation. (e) Comparison between actual and estimated edge orientation corresponding to 4 × 4, 3 × 3 and 2 × 2 areas of the sensor, respectively.

for estimating the edge orientation increased as the area of the sensor decreased. Also from Fig. 9(d) and (e) we observe that as the sensor area decreased, not only the difference between actual and estimated orientation increased but the variance among the different trials also increased. Interestingly, we found that although the MAE obtained by 2 × 2 sensor is 5.88° which is higher than MAE obtained by 4 × 4 sensor (1.67°), yet it is less than the MAE obtained using the neural network based approach (i.e., 7.6°) that used only spatial images for edge orientation detection. This finding highlights the importance of using the spatiotemporal information instead of only spatial information for tactile perception specially when the area of tactile sensor is small.

3.6. Robustness of the method to ridge stimuli

Results presented above were based on the boundary edge of an object with a flat surface. However, in real world scenarios, edges can also appear in the form of ridges on the object's surface. Unlike the boundary edge of an object that occurs at the transition point while palpating from inside of object's surface to outside of object, ridges can occurs within the object's surface as a sudden bump while palpating on the plane surface. Though in both cases i.e., boundary edges and ridges, there exist local discontinuity, the nature of discontinuities are different. To show the robustness of the proposed method in estimating the orientation of ridges, we conducted a separate experiment in which our tactile sensor mounted on the robotic end-effector palpated over the ridged stimuli as shown in Fig. 10(a). We 3D printed 17 ridges oriented at 10° to 90° in a step of 5° on six stimuli bar (3 ridges on each stimuli bar), as shown in the Fig. 10(b)). The palpation procedure was similar to what has been explained in the experimental protocol (Section 2.3), i.e., tactile sensor palpated over the ridge stimuli with a speed of 2 mm/s and the palpation was repeated ten times for each orientation. We calculated the WSS metric for each of the 17 angles of orientation using Eq. (5). To calculate the WSS metric, the spatiotemporal correlation matching was performed between spike images of each ridge orientation and simulated images of 17 different possible ridge orientations, producing 17 different WSS metrics. Subsequently, the actual orientation of ridge was estimated using the Eq. (7). The overall MAE achieved for ridges was 1.97° which is 0.3° more than the overall MAE for the boundary edges (i.e., 1.67°; Table 2). Fig. 11 shows the comparison of MAE obtained for ridges and boundary edges for all the edge orientation. We can see from the figure that the MAE for all the orientations of boundary edges and ridges are comparable. Though there are some variation in MAE for individual edge orientation, yet, we observe similar minimum (0°) and maximum (5°) MAE for both the cases. This result shows that the proposed method is robust to variation in spatial discontinuity due to object's boundary edges or ridges inside the object's surface.

4. Discussion

In this study, we developed a bio-inspired approach to artificially detect edge orientation using neuromorphic encoding of the tactile response generated during active palpation over an object. Inspired by neurophysiological studies mentioned in the introduction [5,23], we converted the analog tactile response to

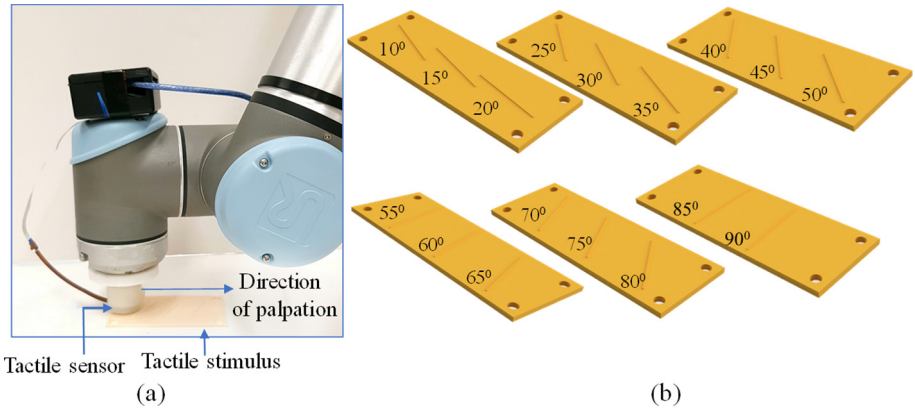

Fig. 10. Experimental setup to estimate the orientation of ridges. (a) Robotic end-effector integrated with tactile sensor and soft layer palpating over the tactile stimulus containing the ridge stimuli. (b) Tactile stimulus bar containing ridges of orientation 10° to 90° with a step of 5°. The height and width of the ridges were 2 mm each.

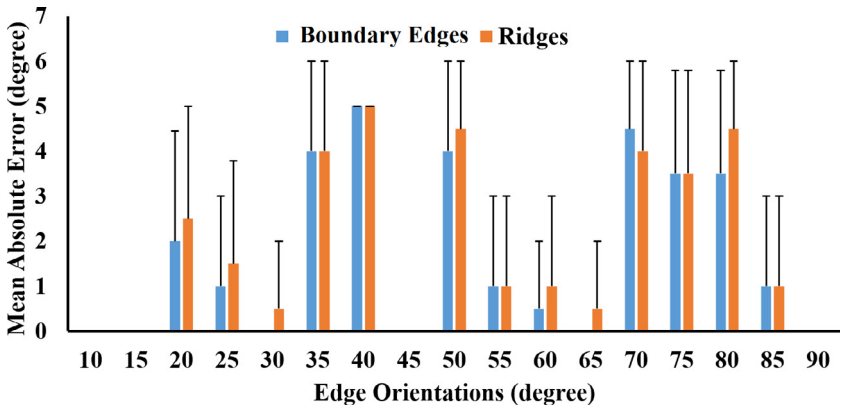

Fig. 11. Errors in edge orientation estimation when tactile sensor palpated over the ridges placed at 17 different orientations.

spike trains that mimic the spatiotemporal nature of the tactile response from first-order tactile neurons. We propose a novel, weighted spatiotemporal similarity (WSS) method that processes spike-based tactile images binned over fixed window-length to decode the edge orientations.

Traditional approaches to detect edges in tactile images uses vision-based edge detection methods [19,21]. However, tactile images differ from vision-based images due to direct physical contact between the tactile sensor and object of interest. An analysing of spike-time distribution of individual taxel demonstrated that tactile response is stochastic in nature, and there exists asymmetry in the tactile response from different taxels. Also, we observed overlapping response from neighboring taxels that makes it difficult to discriminate different orientations of the edge using the tactile response at a single time frame, i.e. when only spatial information was used for edge orientation estimation. On the other hand, such an overlapping tactile response that also occur in human tactile sensing allowing for tactile hyperacuity [40], can be leveraged to discriminate edge orientations that are closely separated by the use of spatiotemporal information processing [41]. The proposed method was able to estimate the edge orientations with overall MAE of 1.67° with an acuity of 5°. Considering the fact that human fingertip can detect edge orientation with an acuity of 3° [23], the result obtained through this study could be a way forward towards efficiently mimicking the human sense of touch. A comparison with supervised classifier networks using spatial and spatiotemporal tactile input showed that the error in edge orientation estimation was 20% lower than its closest counterpart. The proposed method being model-based approach does not need training data, and is computationally less complex. Also, WSS method performs normalized correlation between actual and simulated images which, in theory, makes it an intensity independent method. This is particularly important considering that in an unstructured environment palpation force might vary during the palpation which might generate tactile images with varying intensity. Therefore, in the future we plan to explore applicability of this method for force independent edge orientation detection via palpation.

We demonstrated that even though we are binning the spike-event over the 100 ms duration, our method is sensitive to added noise of 1 ms in spike timing, indicating the importance of temporal resolution to estimate an edge orientation. However, we also observe that the increase in MAE did not increase to significant level unless we introduce spike-time noise of more than 10 ms. This conveys the potential of our method to provides a balanced trade-off between sensitivity and robustness to spike-time noise in edge orientation estimation.

Next, we also showed that even with the spike data corresponding to 60% of total palpation duration, we could estimate edge orientation with a MAE of 2.1° which is 0.34° more than the MAE with full palpation duration. This is mainly important while interacting with a real-world object in real time where it is necessary to detect boundary edges without leaving the object's surface for contour following. Lastly, when developing a tactile system for a robotic/prosthetic hand, the size of the sensor is an important design constraint. Considering this fact, we also looked at the effect of sensor area in estimating the edge orientation. We found that use of spatiotemporal information can provide better edge orientation esti-

mation even with the reduced sensor area (5.2° for 2×2 sensor area) than using only spatial information from larger sensor area (9.4° for 4 × 4 sensor area).

Although the capability of the proposed weighted spatiotemporal similarity metric-based method was demonstrated for edge orientation estimation, there are some limitations of this approach. For example, we tested our method for straight edges only, and the response of this approach to a curved edge is expected to be worse. However, it is an approximation or safe assumption that if the object of interest is sufficiently large compared to the size of the sensor array used, then the current approach can be used to estimate edge orientation. Conversely, for fine objects a higher density sensor array would be needed. Also, this approach assumes that an edge of particular orientation is present in the data and based on this assumption it handles that task as a class estimation problem among predefined simulated edge orientation classes (in this case 17 classes from 10°, 15° . . .90°). This approach is vulnerable during the task where several classes (edge orientations) are not known in advance. Nevertheless, the present study aimed to develop a computational paradigm that is capable of processing spike-based tactile responses for an edge related information. Such a system can help to achieve a high degree of edge orientation discrimination using low-resolution tactile sensors.

5. Conclusion

In this work we presented a novel and robust method, composed of neuromorphic encoding of tactile information and weighted spatiotemporal similarity information for estimating edge orientation. The proposed approaches efficiently leverages spatiotemporal tactile information to aid a low-resolution tactile sensor discriminate edge orientations with very fine precision (±1.67°).

By only encoding normalized temporal changes in tactile information through spikes, the proposed approach demonstrates robustness to common factors of variation present in tactile sensing. Furthermore, by restricting computational modules to only consider sensory changes, the approach showcases bio-inspired computational energy-efficiency while maintaining good performance levels. Such a system represents a step towards developing a tactile sensory feedback module for robotic and prosthetic applications.

CRediT authorship contribution statement

Deepesh Kumar: Conceptualization, Data curation, Formal analysis, Validation, Writing- original draft. **Rohan Ghosh:** Methodology, Formal analysis, Writing-original draft. **Andrei Nakagawa-Silva:** Software, Visualization, Writing-review and editing. **Alcimar B. Soares:** Supervision, Project administration, Writing-review and editing. **Nitish V. Thakor:** Funding acquisition, Recourses, Writing-review and editing.

Declaration of Competing Interest

The authors declare that they have no known competing financial interests or personal relationships that could have appeared to influence the work reported in this paper.

Acknowledgements

The authors would like to thank Anupam K. Gupta, Aravindh N. Swaminathan and Mark Iskarous for many helpful comments, discussions, and suggestion. Also we would like to thank the Office of Naval Research Global and Startup Grant from Singapore Institute for Neurotechnology (SINAPSE), NUS, Singapore for funding this research work.

References

[1] R.S. Johansson, A. Vallbo, Tactile sensibility in the human hand: relative and absolute densities of four types of mechanoreceptive units in glabrous skin, J. Physiol. 286 (1979) 283–300.
[2] S. Chen, Y. Li, N.M. Kwok, Active vision in robotic systems: a survey of recent developments, Int. J. Robot. Res. 30 (2011) 1343–1377.
[3] R.S. Dahiya, M. Valle, Tactile sensing technologies, Robotic Tactile Sensing, Springer, 2013, pp. 79–136.
[4] R.S. Johansson, I. Birznieks, First spikes in ensembles of human tactile afferents code complex spatial fingertip events, Nat. Neurosci. 7 (2004) 170–177.
[5] J.A. Pruszynski, R.S. Johansson, Edge-orientation processing in first-order tactile neurons, Nat. Neurosci. 17 (2014) 1404–1409.
[6] A. Vallbo, R.S. Johansson, et al., Properties of cutaneous mechanoreceptors in the human hand related to touch sensation, Hum. Neurobiol. 3 (1984) 3–14.
[7] R.S. Johansson, J.R. Flanagan, Coding and use of tactile signals from the fingertips in object manipulation tasks, Nat. Rev. Neurosci. 10 (2009) 345–359.
[8] C.M. Oddo, S. Raspopovic, F. Artoni, A. Mazzoni, G. Spigler, F. Petrini, F. Giambattistelli, F. Vecchio, F. Miraglia, L. Zollo, et al., Intraneural stimulation elicits discrimination of textural features by artificial fingertip in intact and amputee humans, Elife 5 (2016) e09148.
[9] S.S. Kim, A.P. Sripati, R.J. Vogelstein, R.S. Armiger, A.F. Russell, S.J. Bensmaia, Conveying tactile feedback in sensorized hand neuroprostheses using a biofidelic model of mechanotransduction, IEEE Trans. Biomed. Circ. Syst. 3 (2009) 398–404.
[10] L.E. Osborn, A. Dragomir, J.L. Betthauser, C.L. Hunt, H.H. Nguyen, R.R. Kaliki, N. V. Thakor, Prosthesis with neuromorphic multilayered e-dermis perceives touch and pain, Sci. Robot. 3 (2018) eaat3818..
[11] W. Lee, J. Cabibihan, N.V. Thakor, Bio-mimetic strategies for tactile sensing, Sensors, IEEE, 2013, pp. 1–4.
[12] S. Sankar, A. Brown, D. Balamurugan, H. Nguyen, M. Iskarous, T. Simcox, D. Kumar, A. Nakagawa, N. Thakor, Texture discrimination using a flexible tactile sensor array on a soft biomimetic finger, in: 18th IEEE Sensors, SENSORS 2019, Institute of Electrical and Electronics Engineers Inc., p. 8956704..
[13] M. Rasouli, Y. Chen, A. Basu, S.L. Kukreja, N.V. Thakor, An extreme learning machine-based neuromorphic tactile sensing system for texture recognition, IEEE Trans. Biomed. Circ. Syst. 12 (2018) 313–325.
[14] U.B. Rongala, A. Mazzoni, C.M. Oddo, Neuromorphic artificial touch for categorization of naturalistic textures, IEEE Trans. Neural Netw. Learn. Syst. 28 (2017) 819–829.
[15] Y. Zhengkun, Z. Yilei, Recognizing tactile surface roughness with a biomimetic fingertip: a soft neuromorphic approach, Neurocomputing 244 (2017) 102–111.
[16] L. Osborn, H. Nguyen, R. Kaliki, N. Thakor, Prosthesis grip force modulation using neuromorphic tactile sensing, in: Myoelec. Controls Symp., pp. 188–191..
[17] R.L. Klatzky, S.J. Lederman, Haptic object perception: spatial dimensionality and relation to vision, Philos. Trans. Roy. Soc. B Biol. Sci. 366 (2011) 3097–3105.
[18] M.A. Plaisier, W.M.B. Tiest, A.M. Kappers, Salient features in 3-d haptic shape perception, Attent. Percep. Psychophys. 71 (2009) 421–430.
[19] C. Muthukrishnan, D. Smith, D. Myers, J. Rebman, A. Koivo, Edge detection in tactile images, in: Proceedings IEEE International Conference on Robotics and Automation, 1987, IEEE, pp. 1500–1505..
[20] T. Tsujimura, T. Yabuta, Object detection by tactile sensing method employing force/torque information, IEEE Trans. Robot. Autom. 5 (1989) 444–450.
[21] N. Chen, R. Rink, H. Zhang, Efficient edge detection from tactile data, in: Proceedings IEEE/RSJ International Conference on Intelligent Robots and Systems. Human Robot Interaction and Cooperative Robots, 1995, IEEE, pp. 386–391..
[22] A.D. Berger, P.K. Khosla, Using tactile data for real-time feedback, Int. J. Robot. Res. 10 (1991) 88–102.
[23] J.A. Pruszynski, J.R. Flanagan, R.S. Johansson, Fast and accurate edge orientation processing during object manipulation, eLife 7 (2018) e31200.
[24] U.B. Rongala, A. Mazzoni, M. Chiurazzi, D. Camboni, M. Milazzo, L. Massari, G. Ciuti, S. Roccella, P. Dario, C.M. Oddo, Tactile decoding of edge orientation with artificial cuneate neurons in dynamic conditions, Front. Neurorobot. 13 (2019) 44.
[25] J.D. Victor, Spike train metrics, Curr. Opin. Neurobiol. 15 (2005) 585–592.
[26] M.v. Rossum, A novel spike distance, Neural Comput. 13 (2001) 751–763.
[27] U.B. Rongala, A. Mazzoni, C.M. Oddo, Neuromorphic artificial touch for categorization of naturalistic textures, IEEE Trans. Neural Netw. Learn. Syst. 28 (2015) 819–829.
[28] E. Satuvuori, T. Kreuz, Which spike train distance is most suitable for distinguishing rate and temporal coding?, J. Neurosci. Methods 299 (2018) 22–33.
[29] W. Gerstner, W.M. Kistler, Spiking Neuron Models: Single Neurons, Populations, Plasticity, Cambridge University Press, 2002.

[30] A.L. Hodgkin, A.F. Huxley, A quantitative description of membrane current and its application to conduction and excitation in nerve, J. Physiol. 117 (1952) 500–544.
[31] R.B. Stein, Some models of neuronal variability, Biophys. J. 7 (1967) 37–68.
[32] E.M. Izhikevich, Simple model of spiking neurons, IEEE Trans. Neural Netw. 14 (2003) 1569–1572.
[33] G. Spigler, C.M. Oddo, M.C. Carrozza, Soft-neuromorphic artificial touch for applications in neuro-robotics, in: 2012 4th Ieee Ras & Embs International Conference on Biomedical Robotics and Biomechatronics (Biorob), IEEE, pp. 1913–1918..
[34] D.R. Lesniak, K.L. Marshall, S.A. Wellnitz, B.A. Jenkins, Y. Baba, M.N. Rasband, G. J. Gerling, E.A. Lumpkin, Computation identifies structural features that govern neuronal firing properties in slowly adapting touch receptors, Elife 3 (2014) e01488.
[35] H. Nguyen, L. Osborn, M. Iskarous, C. Shallal, C. Hunt, J. Betthauser, N. Thakor, Dynamic texture decoding using a neuromorphic multilayer tactile sensor, in: 2018 IEEE Biomedical Circuits and Systems Conference (BioCAS), IEEE, pp. 1–4..
[36] B.P. Delhaye, X. Xia, S.J. Bensmaia, Rapid geometric feature signaling in the simulated spiking activity of a complete population of tactile nerve fibers, J. Neurophysiol. 121 (2019) 2071–2082.
[37] C.W. Zhao, M.J. Daley, J.A. Pruszynski, Neural network models of the tactile system develop first-order units with spatially complex receptive fields, PloS One 13 (2018) e0199196.
[38] P. O'Connor, D. Neil, S.-C. Liu, T. Delbruck, M. Pfeiffer, Real-time classification and sensor fusion with a spiking deep belief network, Front. Neurosci. 7 (2013) 178.
[39] G.E. Hinton, S. Osindero, Y.-W. Teh, A fast learning algorithm for deep belief nets, Neural Comput. 18 (2006) 1527–1554.
[40] J.M. Loomis, An investigation of tactile hyperacuity, Sensory Process. 3 (1979) 289–302.
[41] B.P. Delhaye, X. Xia, S.J. Bensmaia, Rapid geometric feature signaling in the spiking activity of a complete population of tactile nerve fibers, bioRxiv (2018) 461095.

Deepesh Kumar received B.E. degree in Electronics and Telecommunication Engineering from CSVTU Bhilai, India in 2009, and the M. Tech. degree in Electronics and Instrumentation Engineering from the National Institute of Technology Rourkela, India in 2013. He received his PhD degree in Electrical Engineering from the Indian Institute of Technology Gandhinagar, India, in 2018. Currently, he is a Research Fellow at The N.1 Institute for Health, National University of Singapore, Singapore. His main research area includes bio-inspired sensing for robotic and prosthetic applications, technology-assisted neurorehabilitation and bio-medical signal processing.

Rohan Ghosh received the B. Tech. and M. Tech. dual degree in Electronics and Electrical Communication Engineering from Indian Institute of Technology, Kharagpur, India, in 2013 and 2014, respectively. He received his Ph. D. degree from the National University of Singapore, Singapore, in 2018. He is currently a Postdoctoral Research Fellow at The N.1 Institute for Health, National University of Singapore. His main research focuses on computer vision, neural network and neuromorphic algorithms.

Andrei Nakagawa-Silva received the B.S. degree in Mechanical and Biomedical Engineering and an M.Sc. degree in Biomedical Engineering from the Federal University of Uberlandia, Uberlandia, Brazil, in 2012 and 2015, respectively, where he is currently pursuing the Ph.D. degree. His main research focuses on somatosensory system integration and the development and implementing tactile sensing technologies and algorithms for use with robotic and prosthetic limbs.

Alcimar B. Soares received the B. S. degree in Electrical Engineering and the M.Sc. degree in artificial intelligence from the Federal University of Uberlandia, Brazil, in 1987 and 1990, respectively, and the Ph.D. degree in Biomedical Engineering from The University of Edinburgh, U.K., in 1997. He is currently a Full Professor and the Head of the Biomedical Engineering Laboratory, Faculty of Electrical Engineering, Federal University of Uberlandia. His research interests include the modeling and estimation of neuromotor control systems, large-scale neural systems dynamics, targeted neuroplasticity, decoding neural activity, brain-machine interfaces and rehabilitation, and assistive devices. He is also a member of various scientific societies, such as the IEEE Engineering in Medicine and Biology Society, the International Society of Electromyography and Kinesiology, the Brazilian Society of Biomedical Engineering, and the Brazilian Society of Electromyography and Kinesiology. He is the Editor-in-Chief of the Research on Biomedical Engineering journal, the Deputy Editor of the Medical & Biological Engineering & Computing journal, and an Associate Editor of the Journal of Biomedical Engineering and Biosciences.

Dr. Nitish V. Thakor is currently a Professor of Biomedical Engineering, Electrical and Computer Engineering, and Neurology at Johns Hopkins University and directs the Laboratory for Neuroengineering. He is also a Professor at the N.1 Institute for Health (previously known as, Singapore Institute for Neurotechnology (SINAPSE)), National University of Singapore. His technical expertise is in the field of neuroengineering, including neural diagnostic instrumentation, neural microsystems, neural signal processing, optical imaging of the nervous system, neural control of prosthesis, and brain-machine interface. He has authored more than 300 refereed journal publications. He is a Fellow of the American Institute of Medical and Biological Engineering, the Founding Fellow of the Biomedical Engineering Society, and the Fellow of the International Federation of Medical and Biological Engineering. He is a recipient of the Research Career Development Award from the National Institutes of Health and the Presidential Young Investigator Award from the U.S. National Science Foundation. He is also a recipient of the Award of Technical Excellence in Neuroengineering from the IEEE Engineering in Medicine and Biology Society, the Distinguished Alumnus Award from IIT Bombay, Mumbai, India, and a Centennial Medal from the School of Engineering, University of Wisconsin-Madison, Madison, WI, USA. He was the Editor-in-Chief of the IEEE Transaction on Neural Systems and Rehabilitation Engineering. He is presently the Editor-in-Chief of Medical and Biological Engineering and Computing.